PLEASE DISCARD THIS PAGE

Iain MacPherson
Department of Aerospace Engineering,
University of Glasgow,
Glasgow, G12 8QQ, U.K.

PLEASE FIND ATTACHED, PAPER SUBMITTED FOR THE,
27th EUROPEAN ROTORCRAFT FORUM,
PENTIUM CONGRESS CENTRE,
RENAISSANCE HOTEL,
MOSCOW,
RUSSIA

PLEASE FIND ATTACHED, PAPER SUBMITTED FOR THE,
27th EUROPEAN ROTORCRAFT FORUM,
PENTIUM CONGRESS CENTRE,
RENAISSANCE HOTEL,
MOSCOW,
RUSSIA

Abstract

Miniature synthetic jets show promise for the alleviation of a number of flow control problems. Proposed synthetic jet actuators consist of millimetre scale cavities whose oscillatory deformation leads to the alternate intake and ejection of fluid from the surroundings. The current project simulates the operation of synthetic jets using a numerical flow solver.

An investigation of the operation of synthetic jets and their ability to effect flow control is begun with a study of a single synthetic jet actuator issuing into an otherwise still atmosphere. Results of this are compared with previously published data. Simulations are then extended to crossflow conditions to better understand the parameters which are of particular significance for helicopter rotor blade applications.

The project seeks ultimately to simulate the operation of synthetic jet arrays on an aerofoil section. Due to computational constraints however, such an investigation requires that the representation of the jet actuators be simplified. To this end an alternative synthetic jet model has been developed and compared with more detailed CFD simulations.

This simplified jet model has been investigated on an aerofoil undergoing dynamic stall, an application of particular relevance to helicopters.

SYNTHETIC JETS FOR IMPROVED ROTOR PERFORMANCE

I. MacPherson, E.A. Gillies and K.J. Badcock
Department of Aerospace Engineering,
University of Glasgow,
Glasgow, G12 8QQ, U.K.

Abstract

Miniature synthetic jets show promise for the alleviation of a number of flow control problems. Proposed synthetic jet actuators consist of millimetre scale cavities whose oscillatory deformation leads to the alternate intake and ejection of fluid from the surroundings. The current project simulates the operation of synthetic jets using a numerical flow solver.

An investigation of the operation of synthetic jets and their ability to effect flow control is begun with a study of a single synthetic jet actuator issuing into an otherwise still atmosphere. Results of this are compared with previously published data. Simulations are then extended to crossflow conditions to better understand the parameters which are of particular significance for helicopter rotor blade applications.

The project seeks ultimately to simulate the operation of synthetic jet arrays on an aerofoil section. Due to computational constraints however, such an investigation requires that the representation of the jet actuators be simplified. To this end an alternative synthetic jet model has been developed and compared with more detailed CFD simulations.

This simplified jet model has been investigated on an aerofoil undergoing dynamic stall, an application of particular relevance to helicopters.

Notation

b	jet half width(m),
c	aerofoil chord length (m),
h	actuator exit width (m),
k	reduced frequency $(\omega c/2U_\infty)$,
k_h	reduced frequency $(\omega h/2U_\infty)$,
v	(y) velocity component (m/s),
Re	Reynolds Number $(\rho U_\infty c/\mu)$,
Re_h	Reynolds Number $(\rho U_\infty h/\mu)$,
U_∞,Uinf	freestream velocity (m/s),
V_p	peak blowing velocity (m/s),
V cl	centreline velocity (m/s),
Vmean	time averaged velocity (m/s),
δ	boundary layer thickness (m),
ρ	density (kg/m^3),
μ	viscosity (Ns/m^2),
ω	angular frequency $(1/s)$,

Introduction

A number of researchers have shown that steady jets can be used to improve the aerodynamic performance of an aerofoil section. Typically these deliver the jet fluid tangentially (along the surface of the aerofoil) in the direction of the primary flow. Pulsed and oscillatory (i.e. alternate blowing and suction) jets have also been considered for applications such as post-stall reatttachment[1] and lift enhancement[2] and have been found to be more effective than steady blowing for separation control[3].

As a means to effect an oscillatory jet, miniature synthetic or 'zero-mass' jets have the significant advantage that they can be remotely activated using only an electrical supply. This removes the requirement of a pumping system and extensive ducting which is considered a major obstacle for the practical implementation of blowing/suction approaches for aerodynamic flow control on rotorcraft.

Proposed synthetic jet actuators consist of millimetre scale cavities with an opening (or nozzle) to the ambient atmosphere. Oscillatory deformation of the cavity leads to the alternate intake and ejection of fluid from the surroundings. In otherwise stagnant surroundings, a high frequency repetition of this process creates a jet flow from the cavity opening. This is illustrated in figure 1, and has been considered experimentally [4][5][6], and by numerical simulations [5][7][8].

Using a synthetic jet directed radially from the surface of a circular cylinder, Amitay et. al.[9][10] were able to considerably modify the aerodynamic characteristics. Improvements were attributed to the generation of closed recirculating regions which formed at the cylinder surface behind the jet exit. These authors described this as altering the "apparent aerodynamic shape". This mechanism has also been described in subsequent experiments on a thick aerofoil section by the same group[11][12] and has been alluded to by others.

One possible rotorcraft application of synthetic jets is in the alleviation of some of the adverse effects of dynamic stall. Dynamic stall effectively limits a portion of the helicopter flight envelope.

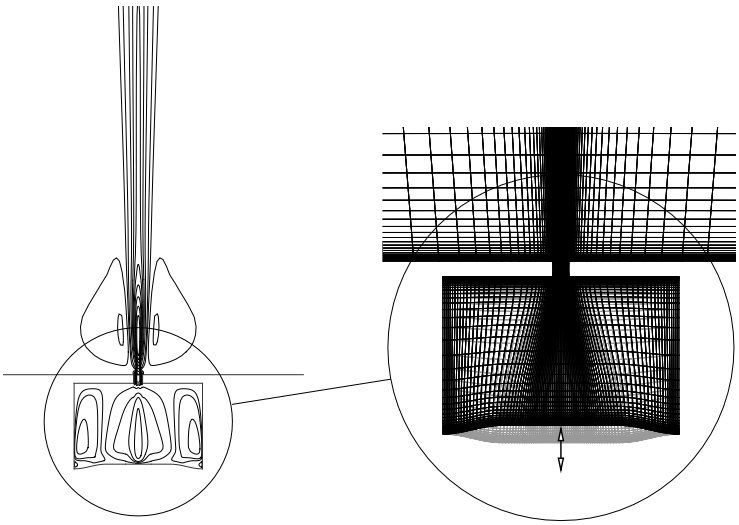

Figure 1: **Jet Flow from a Deforming Cavity**

The loads experienced during this regime are extremely severe and also show considerable hysteresis. It would be desireable, for example, if the large pitching moment excursion, or the negative aerodynamic damping associated with the hysteresis, could be mitigated by synthetic jet actuators placed on the blade. Although the dynamic stall of a helicopter rotor is essentially a three dimensional phenomenon, a useful model of the process is obtained by simulation of a two dimensional blade section undergoing sinusoidal pitching oscillations in and out of the dynamic stall regime [13]. The sinusoidal motion emulates the first harmonic of the rotor blade angle of attack in forward flight. As a preliminary investigation, some of the aerodynamic effects of a synthetic jet actuator placed on a two dimensional aerofoil undergoing oscillatory dynamic stall are presented in this paper.

In order to facilitate this study, a CFD model of a synthetic jet is developed and then implemented on an aerofoil undergoing oscillatory pitching oscillations. All of the simulations presented in the current project utilize the '*pmb2d*' flow solver developed at the the University of Glasgow. This solves the Reynolds-Averaged Navier Stokes (RANS) equations to give a description of the flow behaviour at discrete locations in 2-D space and through time. The computational cost of simulating a synthetic jet flow from a deforming cavity is considerable, as is indicated by the grid detail in figure 1. The complexity of the dynamic stall process also incurrs high computational cost. Therefore, the simulation of dynamic stall combined with the grid detail required for simulation of a deforming cavity is prohibitive for this preliminary study. Instead, a simplified jet model is proposed, which is compared to full CFD models of the jet and cavity, which have in turn been validated against experimental results for single synthetic jets. This simplified jet model may readily be implemented in a dynamic stall simulation, allowing a preliminary flow control study.

Results and Discussion

The aim of the current project is to investigate the effects of a synthetic jet actuator on the stall behaviour of a rotor blade section. The case of a single actuator operating in an otherwise still environment is used for initial validation, since there is little data available for jets issuing into a crossflow.

From the literature, an actuator having an exit width $h = 0.5$ x $10^{-3} m$, operating at 1000Hz and issuing into an otherwise still environment with a peak exit velocity of around 25 m/s emerges as the best test case. A successful simulation of this should provide confidence for a similar model set in crossflow which in turn allows the study of local interactions between the primary (freestream) and jet flows.

The 'pmb2d' flow solver has been developed by the CFD group at the University of Glasgow. This uses a finite volume formulation for the implicit solution of the RANS equations. For

the current calculations, the code uses the two-equation '$k-\omega$' turbulence model. In order to efficiently preserve time-accuracy for unsteady cases, a dual-time method is employed which advances the solution between each real time level using explicit 'pseudo' time marching. The code allows mesh deformation at each real time-step via a modified transfinite interpolation (TFI) method. The cavity geometry used for all of the current work is shown in figure 1. The close-up on the right of the figure illustrates the extremes of cavity floor deflection.

Considering first the case of a jet issuing into a still atmosphere; on the left of figure 1, contours of 'v' velocity demonstrate the production of a jet flow between two vortices. These form out of the separating shear layers produced at the exit edges during blowing. Asides from extensive descriptions of this process, for example references [4],[6] and [8], there are several criteria available for graphical comparison with the existing literature. These mostly consider velocity profiles at the actuator exit and at locations further downstream.

The streamwise (v) velocity at the actuator exit plane, averaged over a complete cycle, is plotted on the left side of figure 2. This shows reasonable agreement with the result of Rizzetta et. al.[8]. Streamwise velocity profiles are plotted on the right of figure 2 at streamwise distances of $y/h = 9.8$ and $y/h = 15.6$ from the jet exit plane. These demonstrate the self similarity of the resulting jet. Although a slight assymmetry can be observed from the figure, synthetic jets under these conditions are broadly stable and symmetrical. For the plots of streamwise velocity shown, data have been normalised with respect to the maximum centreline velocity and the jet 'half width' b (defined as the cross stream distance from the centreline at which the velocity is reduced to half its centreline value) in the fashion of references [7],[4] and [5].

The time variation of centreline velocity at a distance $y/h = 5.0$ downstream from the exit plane is shown on the left of figure 3. On the right, the spatial variation with downstream distance is plotted. Comparison is made with the computational results of Kral et. al.[7], who have shown good agreement with the experiments of Smith and Glezer[4]. The quantative differences in figure 3 indicate that the current jet model has significantly lower jet spreading. Despite this, the broad trends found in the published results are replicated.

Comparison of Jet Models

A crossflow is next applied over the surface in which the actuator is embedded. For intended simulations of jet enabled aerofoils, the detail afforded to the single actuator as has been described above (and in figure 1) is computationally prohibitive. Flow data obtained from the deforming cavity model set in crossflow was thus compared with that from a simplified actuator model. For this simplified model, the cavity and nozzle are removed and a velocity boundary condition is instead imposed at the nozzle exit plane ($y = 0$). The time varying exit velocity used to develop the current results is defined,

$$v(x,t)_{y=0} = V_p \sin^2(2\pi x/h)\sin(\omega t) \quad \text{for} \quad 0 \leq x \leq h$$

Comparison was made in conditions of $Re_h = 350$ and $Re_h = 3500$ using a range of actuation frequencies.

In considering the cavity generated flow, two distinct regimes were observed. At reduced frequency of $k_h = 0.025\pi$, vortices were produced on the downstream side of the actuator and convected in the crossflow direction. At relatively higher reduced frequency ($k_h = 0.1\pi, 0.16\pi$ and 0.25π), these vortices appear to be consumed by a recirculation bubble which becomes established a short distance from the exit. Under identical conditions, these features and behaviour were similarly observed for velocity boundary condition cases and will be discussed further in following subsections.

Flow generated from a deforming cavity is compared with that from an imposed velocity boundary condition for example in figure 4. The instantaneous volume flow rates to and from the simulated cavities are similar, and each case is subject to the same freestream. The comparison therefore highlights the effect of the boundary conditions imposed across the simulated exit orifice. The speed and trajectory of the ejected fluid 'slug' are broadly the same for each case.

Considering here data from the tenth cycle, cavity generated flows were found to be similar to those generated from a sinusoidal velocity boundary condition for reduced frequencies up to $k_h = 0.08\pi$. At $k_h = 0.16\pi$ and $k_h = 0.25\pi$ however, although the cavity flow displays comparable features, the number of cycles required to establish a settled periodic behaviour becomes much greater and no further comparisons were made at higher k_h.

At $k_h = 0.1\pi$, an imposed velocity boundary condition produces a recirculation bubble, whilst vortices from the cavity case continue to be convected individually downstream. Subsequent ve-

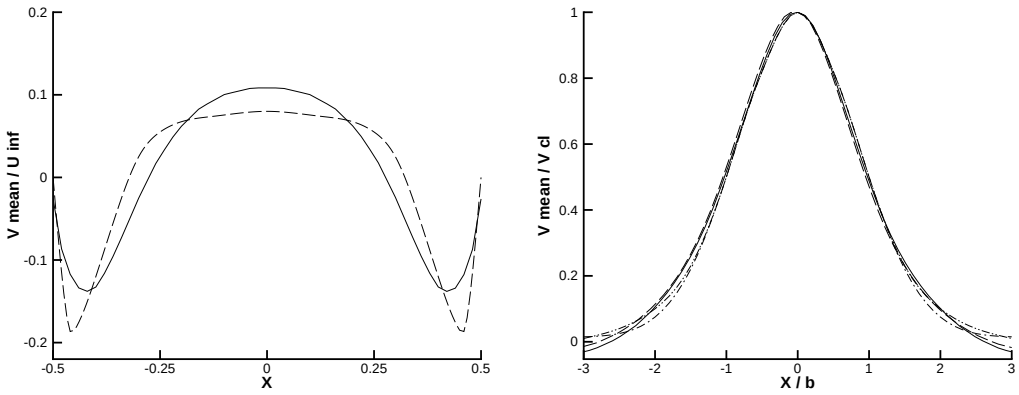

Figure 2: **Streamwise Velocity:**
left, solid line = cycle averaged v velocity at the exit plane, dashed = Rizzetta et. al.(8);
right, cycle averaged v velocity at streamwise stations $y/h = 9.8$ (solid) and $y/h = 15.6$ (dashed), and comparison with Kral et. al(7)

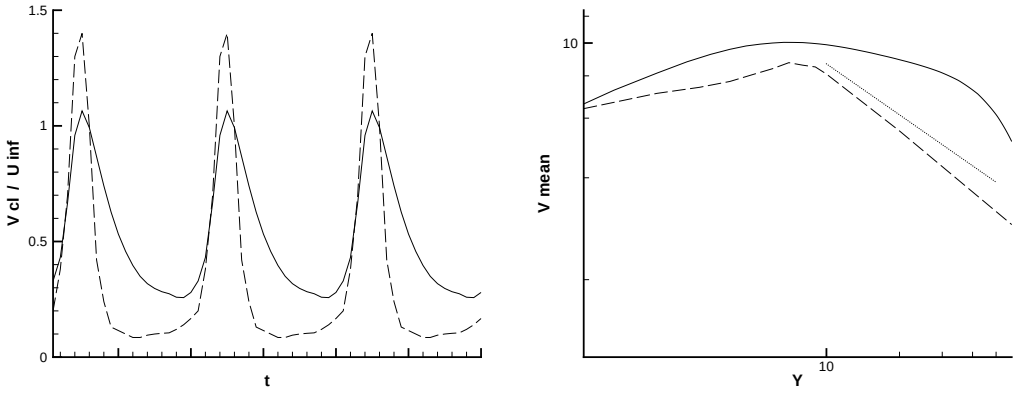

Figure 3: **Centreline Velocity:**
left, solid line = variation with time at $y/h = 5.0$, dashed = Rizzetta et. al.(8);
right, variation of mean velocity with downstream distance, dashed = Kral et. al.(7),
dotted = jet decay rate $\propto (y/h)^{-1/2}$

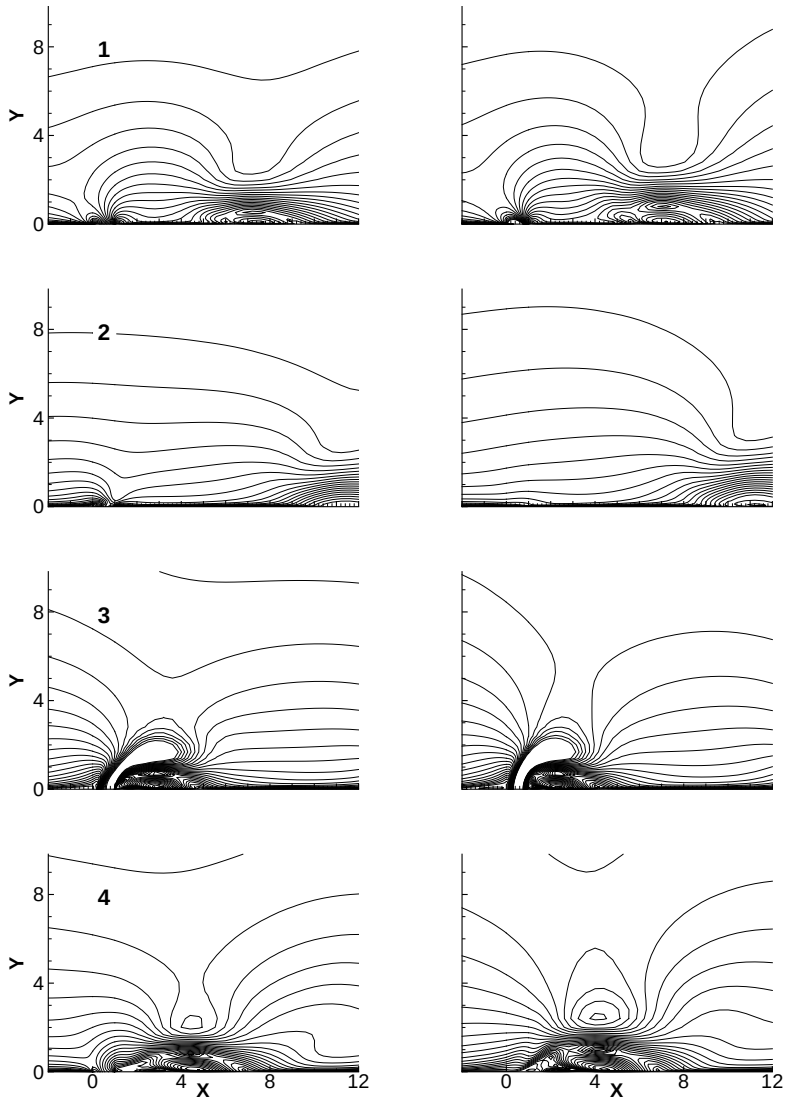

Figure 4: **Comparison of Actuator Models:** velocity magnitude contours at equally spaced instants of an actuation cycle, here $k_h = 0.025\pi$; **left,** flow developed from a deforming cavity (nozzle between $x = 0$ and $x = 1$); **right,** flow developed by imposing a velocity boundary condition, $v(x,t)_{y=0} = V_p \sin^2(2\pi x/h)\sin(\omega t)$ for $0 \le x \le h$

locity boundary condition results (discussed below) indicate that this reduced frequency is close to that where a change of regime occurs. In all comparisons, the assumption of a 'sine squared' profile meant higher peak to peak velocities than those generated from the cavity, thus producing a longer 'slug'. In sympathetic conditions (i.e. within a reduced frequency range), the effect of this may be to establish a permanent recirculation bubble at lower reduced frequencies than is found for the cavity.

Parameter Study

Results of the parameter study discussed in the following sections have been obtained by imposing a 'jet' velocity in place of the deforming cavity. This study considers separately the influence of the blowing magnitude, V_p/U_∞, of Reynolds number Re_h and reduced frequency k_h.

The blowing velocity is found to be crucial in determining the nature of the flow. Three values of V_p/U_∞ were used, 1.0, 2.0 and 3.0 . For $V_p/U_\infty = 1.0$, across the range of Reynolds and reduced frequency considered, such was the magnitude and dissipation of vorticity that vortices generated over each blowing event had disappeared before the beginning of the next. Thus a recirculation region was only established for the two higher values.

For the lowest values of reduced frequency considered here ($k_h = 0.0025\pi$), vortices created during blowing are each individually convected downstream. In crossflow, these are only produced on the downstream side of the actuator. Initially fluid may become entrained even after blowing has ended, such that the actual volume of recirculating fluid continues to increase. This is a short-lived effect however and ultimately, as the vorticity becomes dissipated, the volume of each vortex reduces with downstream distance until there is no recirculating fluid at all.

With increasing reduced frequency ($k_h = 0.0125\pi, 0.025\pi$), the size of the vortices created reduces. In addition to the fact that less fluid is introduced during each blowing cycle (shorter 'slug'), the vortex is less removed from the exit as the orifice suction begins and this impedes any further growth. A point is reached where the suction affects the motion of each vortex away from the actuator ($k_h = 0.05\pi$). This is seen in animations where after the vortex has aquired an initial acceleration, it then slows momentarily as the suction begins, before once again being pulled along by the freestream.

At sufficiently high reduced frequency (above $k_h \approx 0.8$), vortices are no longer carried off downstream, but rather each feeds into a recirculation bubble which becomes permanently established a short distance from the exit. Increasing the reduced frequency beyond that required to create this condition causes the bubble to reduce in size and to move upstream towards the exit. Regions of standing vorticity then exist and counter rotating vortices are produced on the blowing cycle either side of the exit.

The effect of Reynolds number over a range $Re_h = 350$ to $Re_h = 3500$ was also investigated. Being associated with the crossflow, this influences the speed at which vortices are convected downstream. Despite this, for the values of k_h and V_p/U_∞ at which data was obtained, a change of flow regime due to Reynolds number variation was only found for a small number of combinations. From this, when the other parameters are within a critial range, a decreased Reynolds number promotes the establishment of a permanent recirculation bubble.

Amongst the other significant parameters, the boundary layer thickness, δ is also important but has yet to be investigated. The results that have been discussed were obtained in conditions where the nominal boundary layer thickness varied between $\delta \approx 12h$ and $\delta \approx 19h$. This is greater than anticipated at the rotor locations where actuation is proposed. Future work should include an extension of parameter studies to include boundary layer thickness.

Control of Aerodynamic Damping

Having established the validity of imposing a velocity boundary condition to represent flow from a deforming cavity, it was decided to use this approach to simulate jet actuators on a dynamically stalling airfoil.

One of the main adverse effects on a rotor blade entering dynamic stall is the massive increase in nose-down pitching moment. However, the *phasing* of the events during the dynamic stall process can also lead to aeroelastic problems such as stall flutter [14]. Although a rotor blade encounters three-dimensional dynamic stall, the analysis of a two-dimensional aerofoil undergoing harmonic pitching oscillations provides a useful model of a section of rotor blade in forward flight [13].

As the mean angle of attack and amplitude of an oscillating aerofoil is raised, so that the aerofoil enters dynamic stall, the shape of the $C_M - \alpha$ graph changes from a single anti-clockwise loop to a graph with both anti-clockwise and clockwise loops. The coefficient of work done by the

aerodynamic pitching moment over one cycle is,

$$C_W = \oint C_M d\alpha$$

The stability of the aerofoil and rotor blade section is therefore dependent on the direction in which the area of the moment loop is enclosed. An anti-clockwise loop has stable positive torsional damping; whereas a clockwise loop has unstable negative torsional damping. If the total aerodynamic damping over one cycle is low or negative, then there is the possibility of stall flutter of the rotor blade section. Blade stall flutter exerts considerable oscillatory forces on the pitch control linkages of the helicopter and therefore limits a portion of the flight envelope.

Actuation During Deep Dynamic Stall

It was decided to investigate the effects of synthetic jet actuation on the *phasing* of the dynamic stall events during a harmonic pitching oscillation and establish whether such flow control actuation might improve the aerodynamic torsional damping of the rotor blade section.

Following Carta[14] the work done by the aerodynamic pitching moment over one cycle was evaluated from numerical simulations by calculating the area within the $C_M - \alpha$ loops.

The example investigated was a deep dynamic stall case with aerofoil motion governed by $\alpha(t) = 15^o + 10^o \sin(\omega t), k = 0.1$. The Mach number was set at $M = 0.115$, so that the simulation could be validated against available experimental data[15]. The aerofoil used was a NACA0012, represented by a C-type grid having 246 x 49 grid points. A baseline calculation for this case is shown in figures 5 and 6. The model results compare fairly well to oscillatory test data described in reference [15]. As shown in figure 6, the model pitching moment graph has the same topology as the test data, with a stable, unstable and another stable loop. The moment stall point is modelled accurately, as is the timing of dynamic lift increment (although the test data shows a slightly higher maximum dynamic lift). One point to note, however, is that the model predicts a 'pinched' unstable loop, whereas the test data does not show this. This difference between experiment and simulation is within the post stall regime, which is traditionally difficult to model, and also to obtain definitive experimental data for. All other aspects of the experimental $C_L - \alpha$ and $C_M - \alpha$ behaviour are captured by the model.

The $C_M - \alpha$ graph from the computational model shows a stabilizing anti-clockwise loop, S_1, between $5^o < \alpha < 14.3^o$, the appearance of a

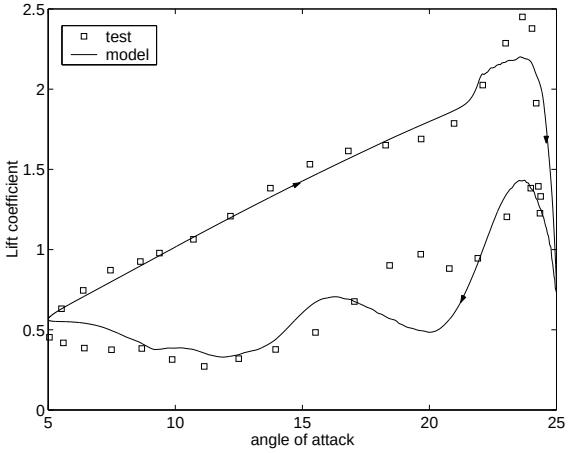

Figure 5: Comparison of test and model data: Lift coefficient

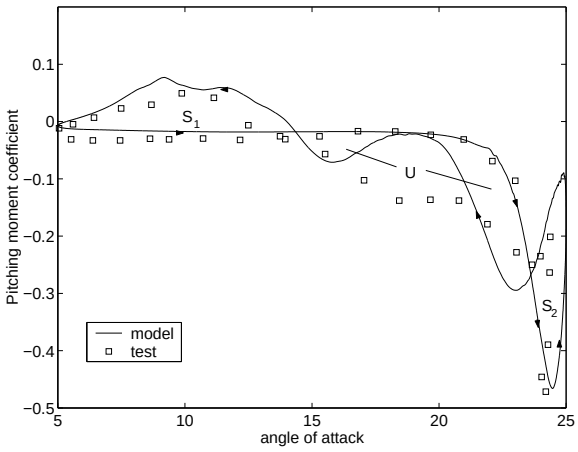

Figure 6: Comparison of test and model data: Moment coefficient

'pinched' clockwise loop, U, between $14.3^o < \alpha < 23.6^o$ which introduces negative torsional damping, and the re-emergence of a final stabilizing anti-clockwise loop, S_2, between $23.6^o < \alpha < 25^o$. The work done by the aerodynamic pitching moment for this case was estimated as $C_W = -0.280$, indicating that, over the full cycle, the rotor blade section is torsionally stable. The C_W value is, however, quite low, due to the clockwise loop U. (It should be noted, however, that the experimental data, which has a larger clockwise loop, indicates slight torsional instability, with $C_W \approx +0.2$.

The same case was investigated with a synthetic jet actuator placed close to the leading edge and on the upper surface of the aerofoil. The jet frequency was set to be 600 times the pitch oscillation frequency, with the jet magnitude described $(V_p/U_\infty) = 0.5$, at a location between $x = 0.0555c$ and $x = 0.0575c$.

The jet actuation is started at the mean incidence angle of 15^o and stopped just after the pitching moment break at 24.4^o. The results of this calculation are shown in figures 7 and 8.

The dynamic lift on the aerofoil is not affected by the jet actuation until around 20^o. The effect of the jet on the lift behaviour is to cause the dynamic lift increment to occur 0.5^o earlier in the cycle, associated with an earlier growth of the dynamic stall vortex. The magnitude and shape of the dynamic lift increment is not significantly changed by the jet actuation. The abrupt loss of lift, associated with the convection of the dynamic stall vortex past the trailing edge, also occurs around 0.3^o earlier in the cycle.

More significantly affected is the pitching moment behaviour. The pitching moment during jet actuation begins to visibly differ from the baseline case at around 17^o. The moment therefore begins to be affected by the jet slightly earlier than the lift. The pitching moment break occurs 0.5^o earlier during the cycle with jet actuation, but the slope of the pitching moment break and its magnitude remain largely unaffected. However, the *re-phasing* of the stall events caused by the jet actuation are seen to have a beneficial effect on the size of the unstable clockwise loop, labelled U in the $C_M - \alpha$ graph. This shrinkage of the unstable region is achieved by the movement of branches 'a' and 'b' marked on figure 8. Branch 'a' of the pitching moment graph is during the period where the dynamic stall vortex is convecting across the aerofoil chord. This branch is well modelled by the simulation so there is confidence that the shrinkage of the unstable region by moving branch 'a' could be achieved by a suitable experimental actuator. Moreover, the stable loop

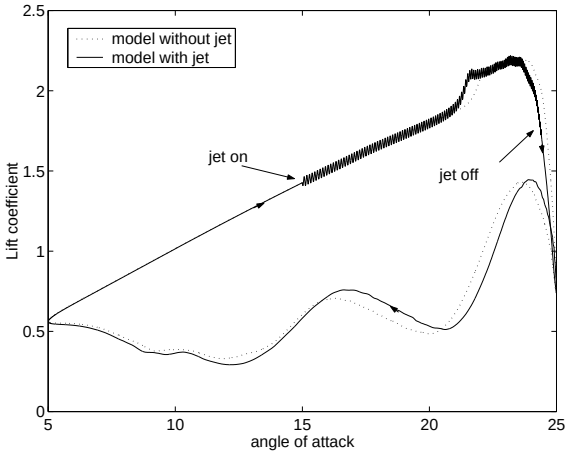

Figure 7: Comparison of model with and without jet: Lift coefficient

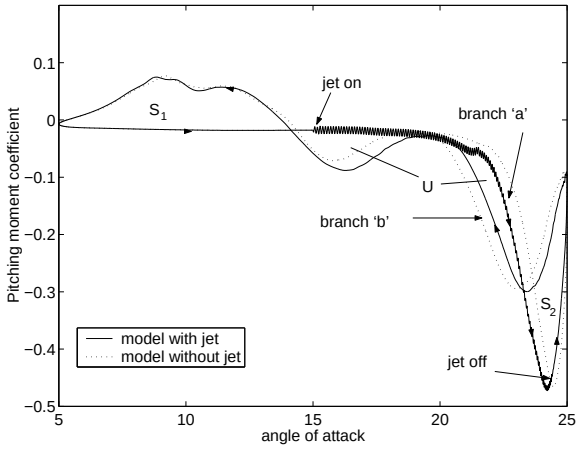

Figure 8: Comparison of model with and without jet: Moment coefficient

S_2 is increased in size by the leftwards movement of branch 'a' resulting from the jet actuation.

The unstable region is also reduced in size by the rightwards movement of branch 'b' in the post-stall regime. This post stall region is much more difficult to simulate and validate (for example the differences between test data and the simulation are most apparent in this region). Whether an actual actuator would have the same effect on this post-stall branch as is shown in the simulation is unclear. However, the simulation suggests that the effect of the jet actuator is to shift this branch to the right; and any rightwards shift of this branch will be beneficial in reducing negative damping.

The stable loop S_1 is largely unaffected by the jet, as one would expect, as no actuation occurs during this part of the cycle.

To estimate the effect of the jet actuation on the cycle torsional stability the work done by the

aerodynamic pitching moment was calculated by integration. The C_M data was filtered to remove the small scale, high frequency variation caused by the jet oscillations. This filtering made little difference to the estimated values for C_W, but made the line integration computationally simpler.

With the jet actuation, the cycle $C_W \approx -0.409$, meaning that the jet *increases* the aerodynamic damping by around 46% and has a beneficial effect on the torsional stability.

In summary, the jet actuation studied here does not diminish the magnitude of the pitching moment break, but the slight re-phasing of the dynamic stall process (e.g. promoting moment stall earlier in the cycle) increases the torsional damping and reduces the likelihood of stall flutter. The magnitude of the dynamic lift is unchanged. The position of the synthetic jet actuator on the aerofoil surface is therefore important— as a jet close to the leading edge is more able to affect the growth of the dynamic stall vortex than actuators further down the aerofoil chord. Indeed, simulations run with the actuator at 40% chord showed little effect.

Another point to consider is that the jet produces a high frequency oscillation in the lift and pitching moment which is in evidence on figures 7 and 8. This oscillation, however, is of quite a small magnitude and very high frequency. It is thought that such oscillations will therefore be highly damped and not detrimental to helicopter vibration.

Actuation During Light Dynamic Stall

On a helicopter rotor there is a wide variation in reduced pitch rate, incidence and Mach number, all of which affect the severity of dynamic stall [14]. An actual rotor application therefore encounters both light and deep dynamic stall. Light dynamic stall is more conducive to stall flutter than deep dynamic stall[16] so it is important to study the effects of a jet actuator on a light dynamic stall case. Very light dynamic stall of a NACA0012 section with $M = 0.1$, $k = 0.1$, $\alpha(t) = 8^o + 8^o \sin(\omega t)$ was investigated using the same synthetic jet as before. The actuation was started at mean incidence and stopped after the pitching moment stall. The actuator promoted the pitching moment break, 'squashing' the unstable $C_M - \alpha$ loop as before in the deep dynamic stall example. However, the strength of the dynamic stall vortex was also considerably increased by the jet actuation. This increase was evident from a much larger dynamic lift increment and a much larger pitching moment break than the original light dynamic stall case. The net effect was a decrease in torsional stability. The increase in both dynamic lift increment and pitching moment break was evident even for very short periods of actuation close to the initial growth of the dynamic stall vortex.

Instead, a different strategy for increasing torsional damping is appropriate for light dynamic stall. The modelling of light dynamic stall is also difficult [16] and the experimental validation data less reliable [15]. This light dynamic stall control strategy is currently under investigation and is the topic of future work.

Conclusions

Synthetic jets are suggested as a means of flow control which may be suitable for use on helicopter rotor blades. In order to validate a synthetic jet model using the 'pmb2d' code, a single actuator issuing into an otherwise still atmosphere has been considered. In regions close to the actuator exit, velocity profiles give reasonable agreement with previously published data . Further downstream however, the lower jet spreading of the current deforming cavity model leads to considerable deviation. The mechanisms by which the jet flow is produced are the same as have been described in the literature. Overall, these results give confidence in a similar model where the actuator has been set in a crossflow.

The flow behaviour produced by a deforming cavity type synthetic jet actuator in a crossflow, was compared with a simpler actuator representation where the actuator exit velocity is imposed without the cavity. Describing the exit velocity with only a simple sinusoidal function; across a practical range of reduced frequency, similar flows were observed for both the simplified and full cavity simulations.

Continuing with the imposed velocity boundary condition model, a parameter study was performed with particular emphasis on Reynolds number Re_h and reduced frequency k_h. At reduced frequencies below $k \approx 0.08\pi$, vortices produced on the downstream side of the actuator, and whose scale decreases with increasing k_h, are individually convected downstream. Increasingly towards $k_h \approx 0.08\pi$, the motion of these vortices is impeded by the suction part of the cycle. Above a critical value, the vortices instead feed into a recirculating region which forms downstream of the actuator exit. Further increases in reduced frequency cause this bubble to reduce in size and to move upstream towards the exit. Across the range of conditions investigated, decreases in Reynolds number were found to pro-

mote the establishment of a recirculating region. An extension of this parameter study to include boundary layer thickness δ is now intended.

A numerical simulation of an airfoil pitching into deep dynamic stall was performed, and calculated aerodynamic coefficients were compared with experimental data. This baseline numerical case gave good agreement over much of the pitching cycle in terms of load magnitudes and in the phasing of events.

Another case was run having a synthetic jet actuator simply represented by a sinusoidal velocity boundary condition, but in all other regards identical to the baseline case. The presence of the jet promoted early growth of the stall vortex, hence pitching moment and lift stall. However, the magnitude of dynamic lift and the α range over which this is maintained was undiminished. Some benefit was identified by the re-phasing of the pitching moment break and subsequent moment recovery. Clockwise loops in $C_M - \alpha$ plots for pitching aerofoils correspond to negative torsional damping associated with the stall flutter phenomena. For the jet enabled aerofoil, the single unstable loop was significantly reduced.

Light dynamic stall is more conducive to stall flutter than deep dynamic stall. A test using identical actuation to that of the deep stall case was unable however, to beneficially alter the aerodynamic damping in a light dynamic stall case. During light dynamic stall, the actuation increased the magnitude of the pitching moment excursion and reduced the aerodynamic damping. Future work will consider alternative strategies for control of light dynamic stall.

References

[1] D. Greenblatt and I. Wygnanski. Dynamic Stall Control by Oscillatory Forcing. *AIAA Paper 98-0676*, 1998.

[2] John F. Donovan, Linda D. Kral, and Andrew W. Cary. Active Flow Control Applied to an Airfoil. *AIAA Paper 98-0210*, 1998.

[3] A. Seifert, T. Bachar, D.Koss, M. Shepshelovich, and I. Wygnanski. Oscillatory Blowing: A Tool to Delay Boundary-Layer Separation. *AIAA Journal*, 31(11):2053–2060, 1993.

[4] Barton L. Smith and Ari Glezer. Vectoring and Small-Scale Motions Effected in Free Shear Flows using Synthetic Jet Actuators. *AIAA Paper 97-0213*, January 1997.

[5] S.G. Mallinson, G. Hong, and J.A. Reizes. Some Characteristics of Synthetic Jets. *AIAA Paper 99-3651*, 1999.

[6] Jose L. Gilarranz, Xue Yue, and Othon K. Rediniotis. PIV Measurements and Modelling of Synthetic Jet Actuators for Flow Control. *Proceedings of FEDSM'98*, ASME Fluids Engineering Summer Meeting (June 21-25), 1998.

[7] L.D. Kral, Donovan J.F., Cain A.B., and Cary A.W. Numerical Simulation of Synthetic Jet Actuators. *AIAA Paper 97-1824*, 1997.

[8] Donald P. Rizzetta, Miguel R. Visbal, and Michael J. Stanek. Numerical Investigation of Synthetic Jet Flowfields. *AIAA Paper 98-2910*, 1998.

[9] Michael Amitay, Andrew Honohan, Mark Trautman, and Ari Glezer. Modification of the Aerodynamic Characteristics of Bluff Bodies Using Fluidic Actuators. *AIAA Paper 97-2004*, 1997.

[10] Michael Amitay, Barton L. Smith, and Ari Glezer. Aerodynamic Flow Control Using Synthetic Jet Technology. *AIAA Paper 98-0208*, 1998.

[11] Barton L. Smith and Ari Glezer. The Formation and Evolution of Synthetic Jets. *Physics of Fluids*, 10(9), September 1998.

[12] M. Amitay, V.Kibens, D. Parekh, and A. Glezer. The Dynamics of Flow Reattachment over a Thick Airfoil Controlled by Synthetic Jet Actuators. *AIAA Paper 99-1001*, 1999.

[13] G.J. Leishman. *Principles of helicopter aerodynamics*. Cambridge University Press, 2000.

[14] F.O. Carta. An Analysis of the Stall Flutter Instability of Helicopter Rotor Blades. *Journal of the American Helicopter Society*, 12(4):1–16, 1967.

[15] R.A.McD. Galbraith, M.W. Gracey, and E.Leitch. Summary of Pressure Data for Thirteen Aerofoils on the University of Glasgow's Aerofoil Database. *University of Glasgow, Department of Aerospace Engineering, Internal Reports*, (9221), June 1992.

[16] J.G. Leishman and T.S. Beddoes. A Semi-Empirical Model for Dynamic Stall. *Journal of the American Helicopter Society*, July 1989.